RADIATION-RESISTANT CERAMICS FOR COMPACT NUCLEAR RAMJETS

Yordan KATSAROV

”Georgi Benkovski” Bulgarian Air Force Academy,(yordankatsarov@gmail.com)

DOI: 10.19062/2247-3173.2026.27.16

Abstract: *This work presents a coupled neutronics-thermal analysis of fuel, advanced ceramic matrix, and coating combinations subjected to a representative short high-power transient. A consistent OpenMC-based workflow was developed to evaluate the impact of beryllium oxide (BeO), silicon carbide (SiC), and zirconium carbide (ZrC) matrices, with and without SiC coatings, on reactivity, radial power distribution, temperature response, and radiation-damage accumulation. The results show that matrix selection dominates the neutronic behavior: BeO systems maintain* k_{eff} *values near unity and exhibit the flattest radial power profiles (6-7 percent variation), while SiC and ZrC matrices produce significantly lower reactivity and increasingly peaked power shapes due to harder neutron spectra. Thermal predictions indicate that all configurations remain within acceptable limits for the imposed transient, though reduced conductivity in SiC and ZrC leads to systematically higher matrix temperatures. Radiation-damage trends follow the same spectral ordering, with BeO systems accumulating the lowest Displacements Per Atom (DPA) and SiC/ZrC matrices experiencing nearly double the damage rates. Overall, the study quantifies the trade-offs between neutronic performance and structural robustness in ceramic systems and provides a physics-based foundation for selecting and optimizing matrix-coating architectures in future high-temperature reactor concepts.*

Keywords: *nuclear ramjet propulsion, radiation-resistant ceramics, high-temperature materials, neutron flux tolerance.*

1. INTRODUCTION

High-temperature ceramics and structural materials are central to the development of advanced nuclear energy and propulsion systems, including high-temperature gas-cooled reactors (HTGRs), microreactors, accident-tolerant fuel concepts, and nuclear thermal propulsion devices. Their ability to maintain structural integrity, thermal stability, and low chemical reactivity under extreme irradiation and temperature conditions makes ceramics attractive candidates for next generation designs operating beyond the limits of conventional metallic systems [1, 2, 3, 4]. In addition to terrestrial power reactors, ceramic-based systems are of particular interest for compact, high-power density nuclear propulsion concepts such as nuclear ramjet engines. Historical programs, most notably the U.S. Project Pluto, demonstrated the feasibility of direct-cycle nuclear ramjets operating at extremely high temperatures and neutron fluxes, where fuel and structural materials were exposed to severe thermal, mechanical, and radiation environments [5, 6]. More recently, renewed interest in nuclear-powered cruise missile concepts, exemplified by the Russian ‘Burevestnik’ system, has further highlighted the need for materials capable of sustaining short-duration, high-power operation under minimal shielding and aggressive thermal conditions [7].

In such systems, material performance during transient operation can be as critical as long-term steady-state behavior. Among candidate ceramic materials, BeO, SiC and ZrC have emerged as leading matrix options due to their high melting points, favorable thermal conductivities, and demonstrated irradiation tolerance [3, 8]. BeO provides strong neutron moderation and low absorption, enabling high reactivity and relatively flat power distributions, while SiC and ZrC offer superior high-temperature strength and chemical stability at the cost of reduced moderation and harder neutron spectra. These materials are also compatible with coated fuel architectures, which have become a cornerstone of advanced reactor and propulsion designs. In parallel, SiC coatings play a critical role in modern ceramic nuclear systems by providing mechanical protection, fission-product retention, and radiation resistance. SiC is a key structural layer in TRISO-derived fuel systems (TRI-Structural Isotropic fuel particles), where it serves as the primary barrier against fission-product release and contributes significantly to overall fuel integrity under high-temperature and irradiation conditions [9]. Extensions of TRISO-inspired coating concepts to nonspherical or pin-type geometries have been proposed for compact reactors and propulsion systems, but their coupled neutronic and thermal impacts remain incompletely characterized. Although significant research has been conducted on ceramic matrices and coatings, the combined effects of neutronics, thermal behavior, and radiation damage related to various ceramic matrix-coating configurations are still not fully understood, especially during short-duration, high-power transients. Matrix composition strongly influences neutron moderation, absorption, and spectral hard ness, which in turn affect reactivity, radial power distribution, and local energy deposition [10]. These spectral effects propagate directly into thermal behavior: reduced moderation typically leads to more peaked power profiles, elevated fuel temperatures, and increased radiation-damage accumulation. For compact systems such as nuclear ramjets and microreactors, where thermal margins are limited and transient operation is intrinsic, understanding these coupled effects is essential for evaluating tradeoffs between neutronic performance and structural robustness. This work develops a consistent OpenMC-based workflow to compare BeO, SiC, and ZrC ceramic matrices with and without SiC coatings under a representative short high-power transient. The methodology integrates Picard-style neutronics thermal coupling at a full power reference state, followed by transient scaling to estimate temperature response and radiation damage accumulation. The analysis focuses on key performance metrics-including effective multiplication factor, radial power distribution, peak fuel temperature, and DPA - to quantify material-dependent behavior across matrix-coating configurations. The results provide a physics-based foundation for selecting and optimizing ceramic fuel architectures in future high-temperature reactor and nuclear propulsion systems.

2. METHODS

This work employs a reproducible Monte Carlo–based workflow to quantify the neutronic, thermal, and radiation-damage behavior of ceramic matrix–coating configurations under a representative short high-power transient. The methodology integrates geometry definition, steady-state neutronics, coupled neutronic–thermal iteration, and transient scaling for DPA estimation.

2.1 Geometry and Material Definition A representative cylindrical U-235 fuel pin surrounded by a non-fissile ceramic matrix and an optional 1.0 mm SiC coating was modeled using OpenMC [11]. Three candidate matrices—BeO, SiC, and ZrC—were selected for their relevance to high-temperature reactor and propulsion applications.

The fuel region was discretized into concentric radial rings to enable spatially resolved tallies of fission power, temperature, and radiation damage. All materials employed temperature-dependent cross sections from ENDF/B-VII.1-based OpenMC libraries.

2.2 Neutronic and Thermal Feedback Quantities

The **effective multiplication factor** k_{eff} is defined as the ratio of neutron population between successive generations, reflecting the balance between neutron production in the fuel and losses through absorption and leakage. In this study, k_{eff} is obtained directly from the Monte Carlo transport calculation and incorporates the combined effects of the fissile fuel, ceramic matrix composition, and temperature-dependent cross sections.

The **fuel temperature** T_{fuel} denotes the volumetric-average temperature within the fissile region, computed using a one-dimensional radial heat-conduction model. It represents the thermal feedback variable that updates temperature-dependent cross sections during each iteration.

2.3 Coupled Neutronic–Thermal Iteration

The neutronic and thermal fields form a closed feedback loop. The ceramic matrix composition and local temperature shape the neutron spectrum, which determines k_{eff} and the spatial fission distribution. In turn, the fission distribution defines the volumetric heat generation that drives the temperature field. Doppler broadening of resonance absorption peaks provides negative reactivity feedback as T_{fuel} increases.

This interaction is resolved using a Picard-style iterative scheme [12]. At each iteration: OpenMC computes ring-wise fission heating; A radial conduction model calculates the updated temperature profile; Temperature-dependent cross sections are regenerated for the next Monte Carlo calculation. Iterations continue until changes in peak T_{fuel} and ring-wise fission power fall below 0.1%, yielding a self-consistent full-power reference state.

2.4 Steady-State Neutronics A steady-state full-power operating point was established using 10^6 active particle histories with sufficient inactive cycles to ensure statistical convergence. From the converged statepoint, k_{eff}, radial fission power, and region-wise reaction rates were extracted. Ring-wise tallies were applied to reconstruct the radial power distribution following standard Monte Carlo practice.

2.5 Transient Scaling and Radiation-Damage Estimation Transient behavior was evaluated using a 30 s linear power ramp followed by a 300 s full-power hold. The converged steady-state fission and damage-energy rates were scaled by the 315 s equivalent full-power duration to estimate accumulated DPA in the fuel, matrix, and coating. Radiation damage was quantified using OpenMC's damage-energy tallies and converted to displacements per atom using the Norgett–Robinson–Torrens (NRT) model [13], a standard comparative metric for irradiation damage.

2.6 Model Scope and Limitations

The thermal model employs one-dimensional radial conduction and neglects axial heat transfer, mechanical deformation, and thermal contact resistance. Irradiation-induced material degradation is not explicitly modeled. The NRT formulation provides comparative, not absolute, DPA estimates. Statistical uncertainties remain non-zero despite large particle histories. The analysis is limited to a single fuel-pin geometry without burnup, fission-product transport, or full-core feedback; however, these omissions do not affect the relative trends among matrix–coating configurations.

3. RESULTS AND DISCUSSION

This section presents the coupled neutronics–thermal response and radiation-damage behavior of BeO, SiC, and ZrC ceramic matrices with and without a 1.0 mm SiC coating under a representative short high-power transient. The key metrics are summarized in Table 1.

Table 1. summary of neutronic, thermal, and radiation-damage metrics for all matrix–coating configurations (315 s equivalent full-power transient).

Case	$\mathbf{k_{eff}}$	$\mathbf{T_{fuel}}$ **(K)**	**Fuel DPA**	**Matrix DPA**
BeO, no coating	1.0596	1326.9	1.13×10^{-5}	8.63×10^{-6}
BeO + SiC (1.0 mm)	1.0436	1331.4	1.16×10^{-5}	8.90×10^{-6}
SiC + SiC (1.0 mm)	0.7393	1352.1	2.07×10^{-5}	1.90×10^{-5}
ZrC + SiC (1.0 mm)	0.7665	1437.6	2.05×10^{-5}	1.69×10^{-5}

3.1 Reactivity and Neutronic Effects. The effective multiplication factor k_{eff} shows strong sensitivity to matrix composition and a secondary dependence on the presence of an SiC coating. The uncoated BeO matrix yields the highest reactivity,
k_{eff} = 1.0596±0.0006,
consistent with BeO's low absorption and favorable moderating properties. Introducing a 1.0 mm SiC coating reduces reactivity to
k_{eff} = 1.0436±0.0007,
corresponding to a penalty of Δk ≈ −0.016 due to replacement of moderating BeO with additional absorbing and scattering material. The SiC and ZrC matrices remain subcritical, with
k_{eff} = 0.7393 and 0.7665,
respectively, reflecting reduced moderation and higher parasitic absorption. Coating effects are smaller for SiC and ZrC, indicating that coatings have the largest neutronic impact when applied to a highly moderating matrix. The reactivity trends are illustrated in FIG. 1.

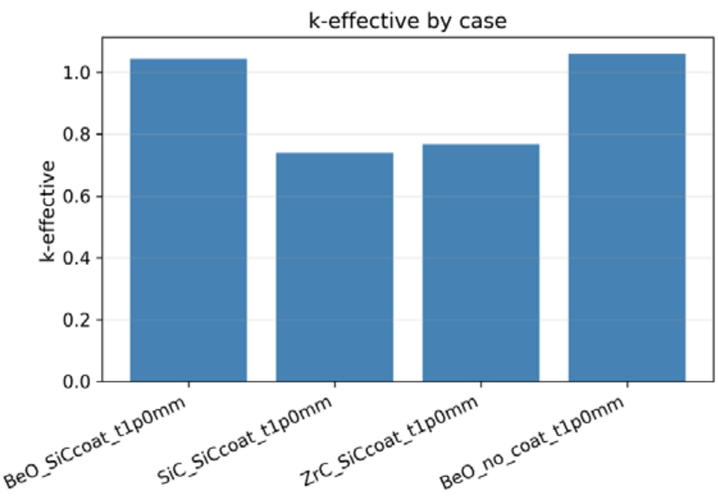

FIG. 1 Reactivity comparison for all matrix–coating configurations.

3.2 Radial Power Distribution and Spectral Behavior. Radial fission power distributions exhibit clear material dependent behavior (FIG. 2). BeO-based systems show the flattest profiles, with only a 6-7% difference between inner and outer fuel rings. Adding an SiC coating introduces mild spectral hardening and increases the center-to-edge ratio to approximately 1.10.

SiC and ZrC matrices produce increasingly peaked profiles, with center-to-edge ratios of approximately 1.18 and 1.22, respectively. These harder spectra shift fission probability toward the core interior, where neutron leakage is lowest. Matrix composition therefore dominates spectral shaping, while the coating introduces a consistent secondary perturbation.

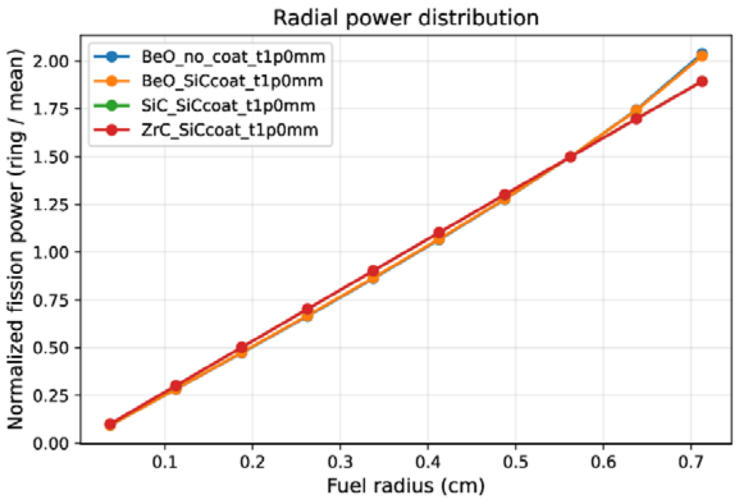

FIG. 2 Radial power distribution for all matrix–coating configurations.

3.3 Thermal Response and Temperature Profiles. All configurations converge to stable thermal states under a 100 kW pin power. BeO-based systems exhibit the lowest peak fuel temperatures:

T_{fuel} = 1326.9 K (BeO), T_{fuel} = 1331.4 K (BeO + SiC).

The SiC coating increases peak fuel temperature by 4-5 K, consistent with its added radial thermal resistance. Fuel temperatures rise for SiC and ZrC matrices:

T_{fuel} = 1352.1 K (SiC), T_{fuel} = 1437.6 K (ZrC),

reflecting their lower thermal conductivity relative to BeO.

Average matrix and coating temperatures follow similar trends, with ZrC-based systems reaching the highest values and BeO-based configurations remaining cooler. Although absolute differences are modest, the systematic increase in temperature for harder-spectrum matrices indicates coupling between neutron spectrum, volumetric heat generation, and thermal transport properties.

Reconstructed radial temperature profiles are shown in FIG. 3, illustrating smooth temperature gradients across the fuel, matrix, and coating regions without sharp interfacial discontinuities.

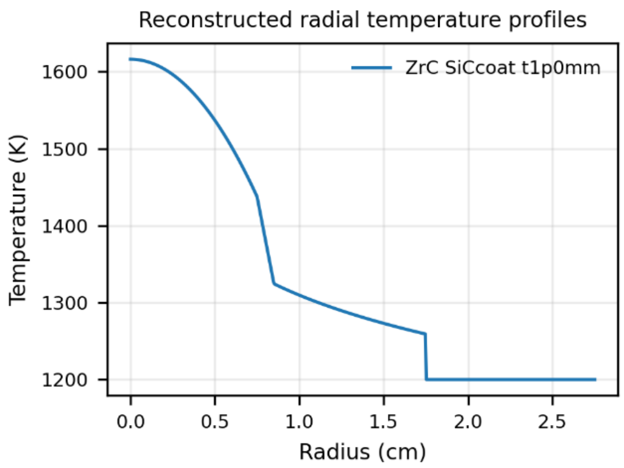

FIG. 3 Reconstructed radial temperature profiles for all configurations.

3.4 Radiation Damage and Damage Partitioning. Radiation damage was quantified using OpenMC damage energy tallies converted to displacements per atom (DPA) via an NRT-style formulation with a displacement threshold energy of E_d = 40 eV. Transient-integrated DPA values were obtained by integrating the damage rate over the 315 s equivalent full-power duration of the ramp-and-hold transient. For the fuel region, the resulting DPA per transient follows the ordering:

$1.13 \times 10^{-5} < 1.16 \times 10^{-5} < 2.07 \times 10^{-5} \approx 2.05 \times 10^{-5}$,

corresponding to BeO, BeO+SiC, SiC+SiC, and ZrC+SiC configurations, respectively. The elevated DPA levels observed in the SiC- and ZrC-based systems are consistent with their harder neutron spectra and reduced moderation, which increase the fast-neutron flux responsible for displacement damage.

Region-resolved DPA results provide further insight into damage redistribution within the composite fuel system. Figure 4 presents the partitioning of transient-induced DPA among the fuel, matrix, and coating regions. For this configuration, radiation damage is strongly concentrated in the fuel, with progressively smaller contributions from the surrounding matrix and the SiC coating. This ordering is physically consistent with neutron transport and material-response characteristics: the fuel experiences the highest fast-neutron flux and contains heavy nuclei with comparatively low displacement energies, while the ceramic matrix and coating materials exhibit higher displacement thresholds and reduced effective damage cross sections.

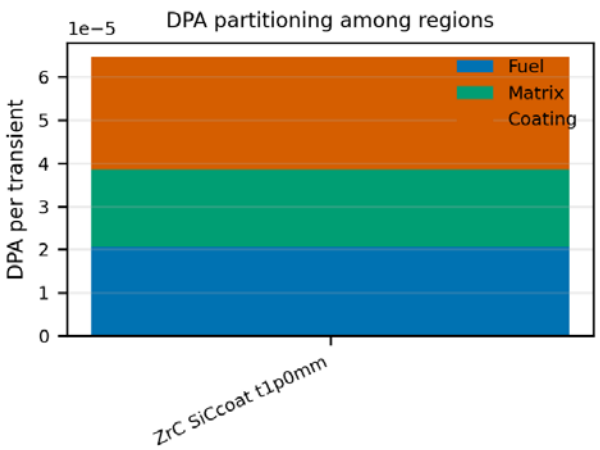

FIG. 4 DPA partitioning among fuel, matrix, and coating regions.

Although matrix DPA remains consistently lower than fuel DPA, the SiC coating accumulates a finite and non-negligible fraction of the total damage, particularly in harder-spectrum systems. The coating contribution remains significantly lower than that of the fuel even under transient conditions, confirming that the thin SiC layer primarily functions as a protective barrier rather than a dominant damage sink. This behavior reflects both the limited coating volume and the attenuation of high-energy neutrons across the fuel-coating interface. Nevertheless, the accumulated coating DPA indicates that radiation damage in protective layers cannot be neglected when assessing long-term structural integrity under repeated transient operation.

Overall, FIG. 4 demonstrates that transient-induced radiation damage is predominantly localized within the fuel, with secondary contributions from surrounding structural ceramics. These findings highlight the importance of region-resolved DPA evaluation when assessing material performance, protective layer effectiveness, and lifetime margins in high temperature, transient-capable reactor concepts. In this context, the NRT model refers to the Norgett–Robinson–Torrens formulation, a classical approach for estimating displacements per atom in irradiated materials.

Although the present study employs OpenMC exclusively, prior multi-code benchmarks reported in the literature demonstrate that modern Monte Carlo transport solvers (e.g., OpenMC, Serpent, MCNP, and Shift) generally exhibit consistent trends in neutron flux spectra and damage-related response functions [14, 15, 16]. While absolute DPA values may vary between codes due to differences in damage-energy treatment, nuclear-data processing, and tally normalization, the relative ordering among fuel, matrix, and coating regions is preserved. This broader agreement supports the physical robustness of the DPA partitioning behavior observed here and reinforces the reliability of the coupled neutronics–thermal methodology.

CONCLUSIONS

The coupled neutronics–thermal assessment performed in this work provides a consistent basis for comparing candidate ceramic matrices and SiC coating configurations under a representative short high-power transient. The results demonstrate that the choice of matrix material remains the dominant factor governing both reactivity and the spatial distribution of deposited energy. BeO-based systems exhibit the highest reactivity, with $\boldsymbol{k_{eff}}$ values near unity even after the introduction of a 1.0 mm SiC coating. Their superior moderation also produces the flattest radial power profiles, limiting peak-to-average variation to approximately 6-7%. In contrast, SiC and ZrC matrices yield substantially lower reactivity and increasingly peaked power shapes, consistent with their harder neutron spectra and higher absorption.

Thermally, all configurations remain within acceptable temperature limits for the imposed full-power transient, though the reduced conductivity of SiC and ZrC matrices leads to systematically higher fuel temperatures. The addition of a SiC coating introduces only a modest thermal penalty relative to the matrix effect itself. Radiation-damage trends follow the same spectral ordering: BeO systems accumulate the lowest DPA in both fuel and matrix regions, while SiC and ZrC matrices experience nearly a factor-of-two increase in damage rates.

Overall, the results highlight a clear trade-off between neutronic performance and structural robustness. BeO provides the most favorable neutronic environment but requires careful consideration of its mechanical and manufacturing constraints. SiC and ZrC offer superior structural resilience but impose significant reactivity penalties that must be compensated elsewhere in the core design.

These findings provide a quantitative foundation for selecting and optimizing ceramic matrix–coating combinations in advanced high-temperature reactor concepts, and they motivate future work incorporating full-core geometry, burnup effects, and experimentally validated thermal-mechanical models.

Future extensions of this work will focus on expanding the modeling framework to full-core geometries and incorporating burnup-dependent spectral evolution. Coupling with validated thermal–mechanical models will enable assessment of stress development, coating integrity, and swelling behavior under repeated transient loading.

AKNOWLEDGMENT

The author gratefully acknowledges the support of the Department of Aviation Equipment and Technologies at the Bulgarian Air Force Academy for providing the computational resources and institutional support necessary for this work. The author also thanks colleagues for valuable discussions and technical feedback that contributed to the development and interpretation of the results.

REFERENCES

[1] M. P. Short, et al., Materials challenges for nuclear systems, *Annual Review of Materials Research*, vol. 49, pp. 1–33, 2019;

[2] R. Konings and A. H. H. Janssen, Nuclear fuel materials, in *Comprehensive Nuclear Materials*, 2nd ed., Elsevier, 2020;

[3] Y. Katoh, et al., Radiation effects in SiC for nuclear structural applications, *Journal of Nuclear Materials*, vol. 499, pp. 471–486, 2018;

[4] G. R. Odette, M. J. Alinger and B. D. Wirth, Recent developments in irradiation-resistant steels, *Annual Review of Materials Research*, vol. 38, pp. 471–503, 2008;

[5] T. A. Heppenheimer, The nuclear ramjet: Project Pluto, *IEEE Spectrum*, vol. 38, no. 9, pp. 44–49, 2001;

[6] J. L. Anderson, Nuclear propulsion concepts for atmospheric flight, *Journal of Propulsion and Power*, vol. 19, no. 3, pp. 347–356, 2003;

[7] D. Wright, Russia's nuclear-powered cruise missile, *Bulletin of the Atomic Scientists*, vol. 75, no. 2, pp. 61–67, 2019;

[8] J. H. G. van der Laan, Advanced ceramic materials for nuclear applications, *Journal of Nuclear Materials*, vol. 494, pp. 1–11, 2017;

[9] D. A. Petti, et al., TRISO-coated particle fuel performance, *Nuclear Engineering and Design*, vol. 222, pp. 281–297, 2003;

[10] J. J. Duderstadt and L. J. Hamilton, *Nuclear Reactor Analysis*, Wiley, New York, USA, 1976;

[11] P. K. Romano, et al., OpenMC: A state-of-the-art MC code for research and industry, *Annals of Nuclear Energy*, vol. 82, pp. 90–97, 2015;

[12] A. T. Godfrey, et al., Coupled MC analysis for high-temperature reactor systems, *Nuclear Technology*, vol. 203, pp. 1–15, 2018;

[13] M. J. Norgett, M. T. Robinson and I. M. Torrens, A proposed method of calculating displacement dose rates, *Nuclear Engineering and Design*, vol. 33, pp. 50–54, 1975;

[14] MIT Computational Reactor Physics Group, Collection of Models for Reactor Physics Benchmarks, available at: https://github.com/mit-crpg/benchmarks, accessed on 19 Feb. 2026;

[15] A. Valentine, UKAEA Benchmarking of the Serpent-2 Monte Carlo Code for Fusion Applications, 2019. Available at: https://serpent.vtt.fi/mtg/2019_Atlanta/Valentine1.pdf (serpent.vtt.fi in Bing), accessed on 19 Feb. 2026;

[16] ReactorMC, MCNP, OpenMC & Serpent Tutorials, available at: https://reactormc.net/, accessed on 19 Feb. 2026.